



<b>Title</b>	A Radial Clutch Needle for Facile and Safe Tissue Compartment Access
<b>Authors(s)</b>	O'Cearbhaill, Eoin D., Laulicht, Bryan, Mitchell, Niamh
<b>Publication date</b>	2019-12
<b>Publication information</b>	O'Cearbhaill, Eoin D., Bryan Laulicht, and Niamh Mitchell. "A Radial Clutch Needle for Facile and Safe Tissue Compartment Access" 2, no. 5-6 (December, 2019).
<b>Publisher</b>	Wiley
<b>Item record/more information</b>	<a href="http://hdl.handle.net/10197/11266">http://hdl.handle.net/10197/11266</a>
<b>Publisher's statement</b>	This is the peer reviewed version of the following article: O'Cearbhaill, E. D., Laulicht, B. , Mitchell, N. , Yu, L. , Valic, M. , Masiakos, P. and Karp, J. M. (2019), A Radial Clutch Needle for Facile and Safe Tissue Compartment Access. Medical Devices Sensors, which has been published in final form at <a href="https://doi.org/10.1002/mds3.10049">https://doi.org/10.1002/mds3.10049</a> . This article may be used for non-commercial purposes in accordance with Wiley Terms and Conditions for Self-Archiving
<b>Publisher's version (DOI)</b>	10.1002/mds3.10049

Downloaded 2023-10-06T13:54:56Z

The UCD community has made this article openly available. Please share how this access benefits you. Your story matters! (@ucd\_oa)



© Some rights reserved. For more information

DOI: 10.1002/((please add manuscript number))

**Article type: Communication**

**Title: A Radial Clutch Needle for Facile and Safe Tissue Compartment Access**

*Eoin D. O’Cearbhaill<sup>1-4\*</sup>, Bryan Laulicht<sup>1,2,4</sup>, Niamh Mitchell<sup>3</sup>, Lawrence Yu<sup>1,2</sup>, Michael Valic<sup>1,2</sup>, Peter Masiakos<sup>4,5</sup>, Jeffrey M. Karp<sup>1,2,4,6,7\*</sup>*

<sup>1</sup> Center for Nanomedicine, Division of Engineering in Medicine, Department of Medicine, Brigham and Women’s Hospital, Cambridge, MA 02115, USA

<sup>2</sup> Harvard - MIT Division of Health Sciences and Technology, Cambridge, MA 02139, USA

<sup>3</sup> School of Mechanical and Materials Engineering, UCD Centre for Biomedical Engineering, and UCD Conway Institute of Biomolecular and Biomedical Research, University College Dublin, Belfield, Dublin 4, Ireland.

<sup>4</sup> Harvard Medical School, Boston, MA 02115

<sup>5</sup> Department of Pediatric Surgery, Massachusetts General Hospital, Boston, MA 02114

<sup>6</sup> Broad Institute of Harvard and MIT, Cambridge, Massachusetts, 02139, USA

<sup>7</sup>Harvard Stem Cell Institute, 1350 Massachusetts Avenue, Cambridge, Massachusetts 02138, USA

E-mail: eoin.ocearbhaill@ucd.ie; jeffkarp.bwh@gmail.com

Keywords: medical devices, safety needles, minimally invasive, cannulation, bioinspiration

This article has been accepted for publication and undergone full peer review but has not been through the copyediting, typesetting, pagination and proofreading process, which may lead to differences between this version and the [Version of Record](#). Please cite this article as [doi: 10.1002/MDS3.10049](https://doi.org/10.1002/MDS3.10049)

This article is protected by copyright. All rights reserved

## **Abstract**

Efficient and safe access to targeted therapeutic sites is a universal challenge in minimally invasive medical intervention. Percutaneous and transluminal needle insertion is often performed blindly and requires significant user skill and experience to avoid complications associated with the damage of underlying tissues or organs. Here, we report on the advancement of a safer needle with a radial mechanical clutch, which is designed to prevent overshoot injuries through the automatic stopping of the needle once a target cavity is reached. The stylet-mounted clutch system is inexpensive to manufacture and compatible with standard hypodermic or endoscopic needles, and therefore can be adapted to achieve safe access in a myriad of minimally invasive procedures, including targeted drug delivery, at-home and in-hospital intravenous access, laparoscopic and endo- and trans-luminal interventions. Here, we demonstrate the clutch needle design optimization and illustrate its potential for rapid and safe minimally invasive cannulation.

## **Introduction**

Percutaneous access is the hallmark of minimally invasive intervention, with most procedures starting with hypodermic needle insertion, with or without image guidance. There are a vast number of procedures requiring percutaneous needle insertion, such as biopsies [1] and brachytherapy [2], epidural [3] and regional anesthesia [4] administration, vascular access [5] (including hemodialysis [6] and blood sampling [7]), intra-articular injection [8], and laparoscopy [9] that still rely on a high-degree of user skill. In laparoscopic access, common to many minimally-invasive surgical interventions, major complications, such as perforation of larger blood vessels or the bowel, are frequently associated with the initial phase of trocar insertion (rates of 0.04% [10] - 0.18% [9] have been reported, but actual incidences may be much higher [11]). It has been noted that 30%-50% of bowel injuries and 13%-50% of vascular injuries are not detected during procedures, leading to high rates of morbidity and mortality.[12] The risks are so significant that there has been a shift from what was the standard in closed laparoscopic access, with the sub-optimal Veress needle, towards more invasive open techniques which involve blunt tissue dissection.[13] However, a recent Cochrane report has found no evidence in reduction of risks of these life-threatening visceral and vascular injuries when closed entry techniques were

replaced by open approaches.[14] Similarly, internal tissue or compartment access in endoscopic [15] or transluminal-based procedures (e.g. natural orifice transluminal endoscopic surgery) [16] is often achieved through remotely deployed spring-loaded or direct insertion techniques that offer poor haptic feedback and hence user-dependent performance.

Since its first use in the mid-19th century to treat neuralgia, [17], the hypodermic needle has been the physician's primary tool in performing minimally invasive interventions. While the materials used and methods of manufacturing have been refined and new forms of assistive imaging have been developed, the mode of cavity-targeting needle insertion has remained largely the same; namely, the user inserts a needle until they sense a drop off in resistance (often in combination with visualization) and use muscle memory to rapidly stop the needle and avoid creating through-and-through puncture injuries. Intuitively, complication rates associated with needle insertion are heavily influenced by the user's experience and training [18]. Clinicians rely heavily on anatomical locations and manual haptic feedback during placement, however target visibility, target access and tool maneuverability are all key issues, constraining the precision and accuracy of needle placement [19]. This can result in an increased risk of complications during a healthcare practitioner's learning curve or in emergency situations.

As summarized by van Gerwen et al. [20], needle insertion speeds can range dramatically, from 0.4mm/s to 10mm/s in epidurals [21], with speeds ranging from 1 mm/s – 1,000mm/s at different stages of needle insertion in brachytherapy [22]. Furthermore, maximum needle insertion forces measured in vivo during brachytherapy procedures displayed high levels of variability (3.34 - 13.94N for 18Ga and 13.87 - 19.11N for 17Ga needles) [23]. It is therefore unsurprising that conventional manual control of needle insertion can lead to highly variable results [24]. Several research groups have tried to modify or improve the conventions of needle insertion through novel mechanical mechanisms [25], modifying the Veress needle [26], multi-component actuation inspired by burrowing mechanism of ovipositing wasps [27], or using robotic-assisted surgical tools are expensive [28], however many of these approaches lack the simplicity and versatility to facilitate widespread adoption.

Here, we describe the development of a radial clutch needle (clutch needle) for percutaneous soft tissue access. The concept of a mechanical clutch was originally proposed by Bassett et al. [29], where unlike conventional needle insertion, the user pushes a stylet inside a serpentine-shaped needle that locks with and advances the needle in response to resistance at the



distal tip of the device and disengages safely once a target cavity is reached. However, there were a number of issues related to the original serpentine-shaped needle design that inhibited clinical translation. The design suffered from (1) manufacturing scalability challenges in a highly cost-competitive market, (2) the clutch deployment relied on a somewhat unpredictable buckling mechanism which could result in plastic deformation of the stylet and repeatability issues, and (3) aesthetically, the device's large footprint was off-putting for users and patients. To facilitate widespread adoption, a design is required that would be universally compatible with existing hypodermic, endoscopic and laparoscopic techniques and cylindrically-shaped needles, possessing a clutch mechanism that behaves elastically and repeatability.

Muscle contraction and elongation provide template examples of structures in nature, which can store elastic energy to be released on demand. An example of such a muscle operating within a cylindrical constraint of a skeleton, similar to the internal body of a needle, is the chameleon's tongue. Here, once triggered, the muscle is released from a constrained configuration and frictionlessly elongates into a relaxed, axially-extended conformation. Throughout this process, collagen fibers wound helically within this muscle extend axially, propelling the tongue forward. Structurally, these helically wound fibers behave as biaxial braids and this conformation change is analogous to braided medical devices that are designed to undergo conformation changes to facilitate radial expansion after low profile delivery (e.g. stents [30]) or to grow axially (e.g. pediatric devices [31]). Here, we propose a design inspired by this mechanism, creating an elastically deformable radial clutch mounted to a stylet that engages with the inner wall of standard needles when the stylet is compressed axially when registering a resistive force above a specified threshold at the needle tip (**Figure 1**).

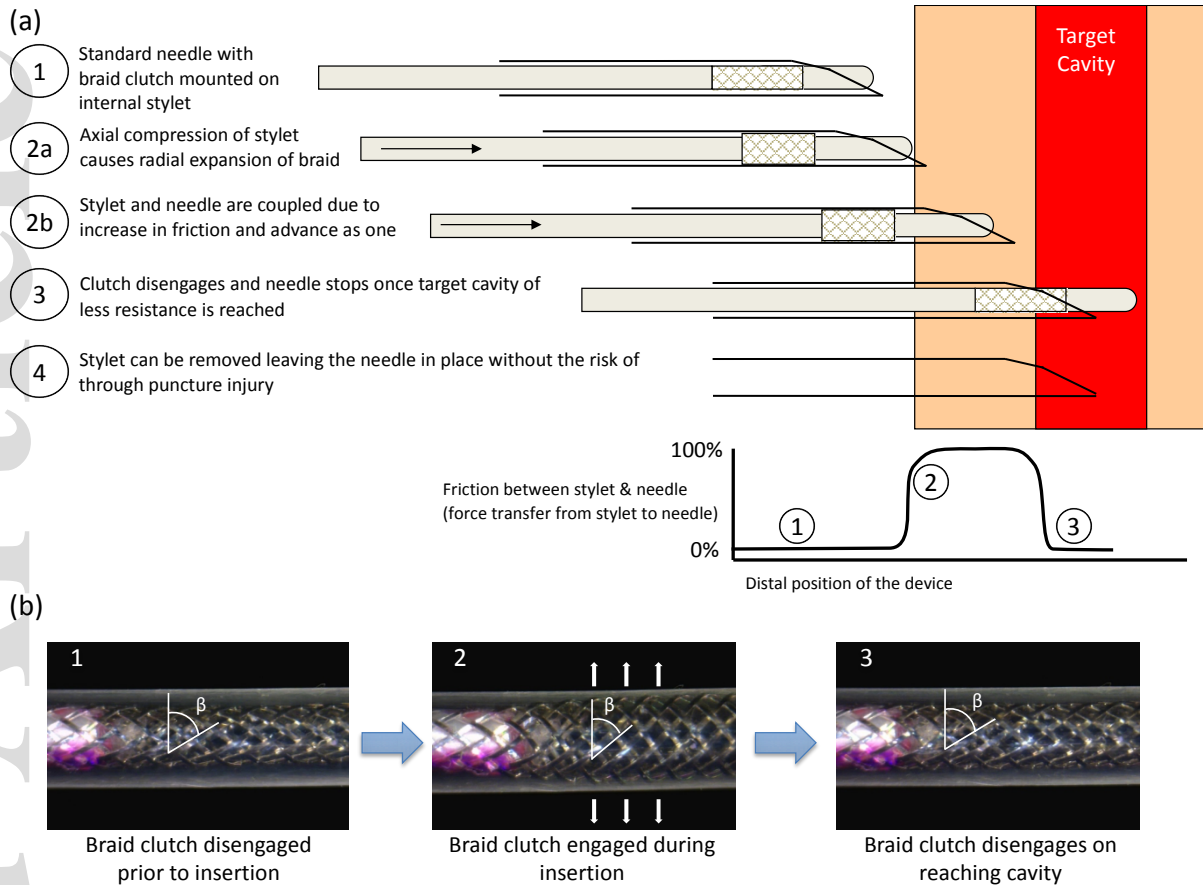


*Figure 1: Device Concept (a) An overview of the principle of placing the needle in a target site using a radial clutch-based mechanism. (1) The mechanical clutch needle assembly comprises a braid mounted to a blunt rounded-tip stylet to form the radial clutch and a standard double-beveled needle. When the assembly is unloaded there is no friction between the stylet and the needle; (2a) Once the needle tip is approximated against the tissue surface, only the stylet is pushed. As the stylet is blunt it does not penetrate the tissue and thus axial force translates to radial expansion of the braid until it creates a frictional interlock with the needle; (2b) Once sufficient force has been transferred to the needle, the stylet and needle are coupled and advance as one; (3) When a drop off in resistance occurs on entering the target cavity, the stylet-mounted clutch disengages from the needle and only the blunt stylet continues to advance; (4) At this point the stylet can be retract or a guidewire inserted prior to safe needle removal. (b) A representative image of the braid-based radial clutch being deployed in a transparent tube for ease of visualization. When axial compression is applied to stylet (1 -> 2), the initial braid angle  $\beta_1$  becomes more acute as the braid expands radial until the helical-wound wires come into contact*

with the needle body  $\beta_2$ . When axial compression is released (3),  $\beta_2$  returns to  $\beta_1$  and the stylet is free to move without friction inside the needle body.

To demonstrate proof-of-principle, an industry standard low PPI (crossings or picks per inch) flat-wire stainless steel biaxial braid was crimped to the mid-portion of a sectioned stylet obtained from a dismantled Veress needle (**Figure 2**). The theoretical and bench-top performance of the system are evaluated and optimized prior to testing prototype devices in simulated clinical scenarios.

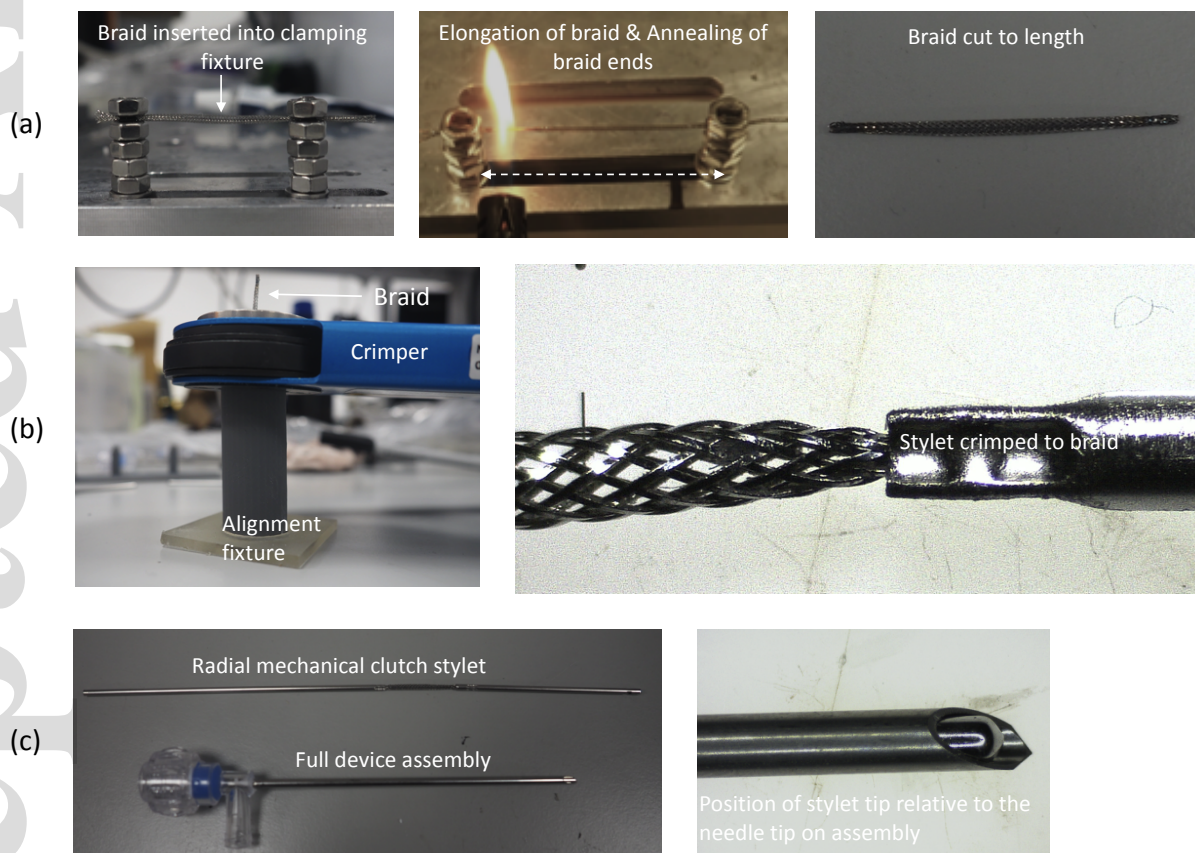


**Figure 2:** Device assembly (a) Braid preparation. A flat-wire stainless steel biaxial braid with a low number of crossings per inch ( $\sim 30 - 40$  PPI) is rough cut to  $\sim 55$ mm length, to provide excess material for a final target clutch length of 40.5mm. The braided wire segments are stretched in a rig so that the ends can be annealed and cinched to prevent the wire unravelling and to aid insertion into the stylet body. Annealing is performed locally using an open flame for  $\sim 10$  seconds until it glows red and the braid is cut to its final length at the annealed points' (b) The braid is

*inserted at either end into two halves of a stylet from a disassembled Veress Needle. An alignment fixture in combination with a hand crimping tool (DMC AF8) is used to control the point of crimping. Care is taken to ensure that the crimp location does not increase the profile of the stylet;*

*(c) The stylet is inserted into a matching standard double-bevel needle. Optionally, a Tuohy-Borst adapter (which contains an adjustable hemostatic valve), can be adhered to the proximal end of the needle and the valve tightened onto the needle to lock the relative position of the stylet and needle until the mechanical clutch system is ready for use.*

The mechanical behavior of biaxial braids on deformation is predictable and has been previously modeled by Jedwab et al. to predict the performance of self-expanding stents, [32] where each wire is modeled as an open-coiled helical spring as described by Wahl [33]. Here, we adapt this model to illustrate how the sensitivity of the clutch engagement can be tailored to coincide with a specific resistive force sensed at the distal end of the stylet and thus tailored to different applications based on the resistance offered by the tissue (**Figure 3(a)**). Assuming minimal frictional losses between the wires, this mathematical model effectively captures the impact of varying the braid angle up to the point at which the inner diameter of the needle is contacted. Due to complexity of the contact between the braid and the needle, their subsequent interaction is examined experimentally. A custom set-up can be used to illustrate clutch sensitivity experimentally (**Figure 3(b)**). Here, the stylet was inverted in the needle and fixed at its proximal end to a stage, so that free hanging weights can be attached to the proximal end of the needle to simulate different levels of tissue resistance. The needle was attached to a load cell which can track the amount of force transmitted by the stylet-mounted clutches to the needle in response to this static loading. As expected with gradually increasing PPI count (from 30 to 50 PPI), the clutch sensitivity decreases, illustrating the tunability of the system. The most densely wound braid (50 PPI) does not undergo enough radial expansion to engage with the needle and would therefore be an ineffective clutch. To demonstrate the elasticity and repeatability of the clutch engagement mechanism, a similar dual-load cell set-up to that employed by Bassett et al. [29] is used (**Figure 3(c)**) to test an optimized device. In cyclic testing, the input force ( $F_{in}$ ) upon simulating pushing of the stylet is compared to the output force ( $F_{out}$ ) at the distal end of the stylet, with a clutch designed to engage at tissue resistance forces above 1N. The plateau of the  $F_{out}$  at ~3-4N indicates that over a range of application forces ( $F_{in}$  up to 12N), the clutch remains locked and any

additional force will be transferred to needle, facilitating needle advancement. Next, in a benchtop model of closed laparoscopic access, clutch needles were compared to current clinical practice gold-standard Veress needles in a side-by-side comparison (**Figure 3(d)**), where an inflated latex balloon was used to represent an underlying organ or blood vessel that could be damaged through needle overshoot. In simulated use cases by an unskilled user and controlled test conditions where the needles were attached to a uniaxial test rig, there were no reported incidences of balloon puncture for the mechanical clutch needle. However, in the controlled displacement control test, balloon puncture occurred in 8 out of 10 cases using the Veress needle.

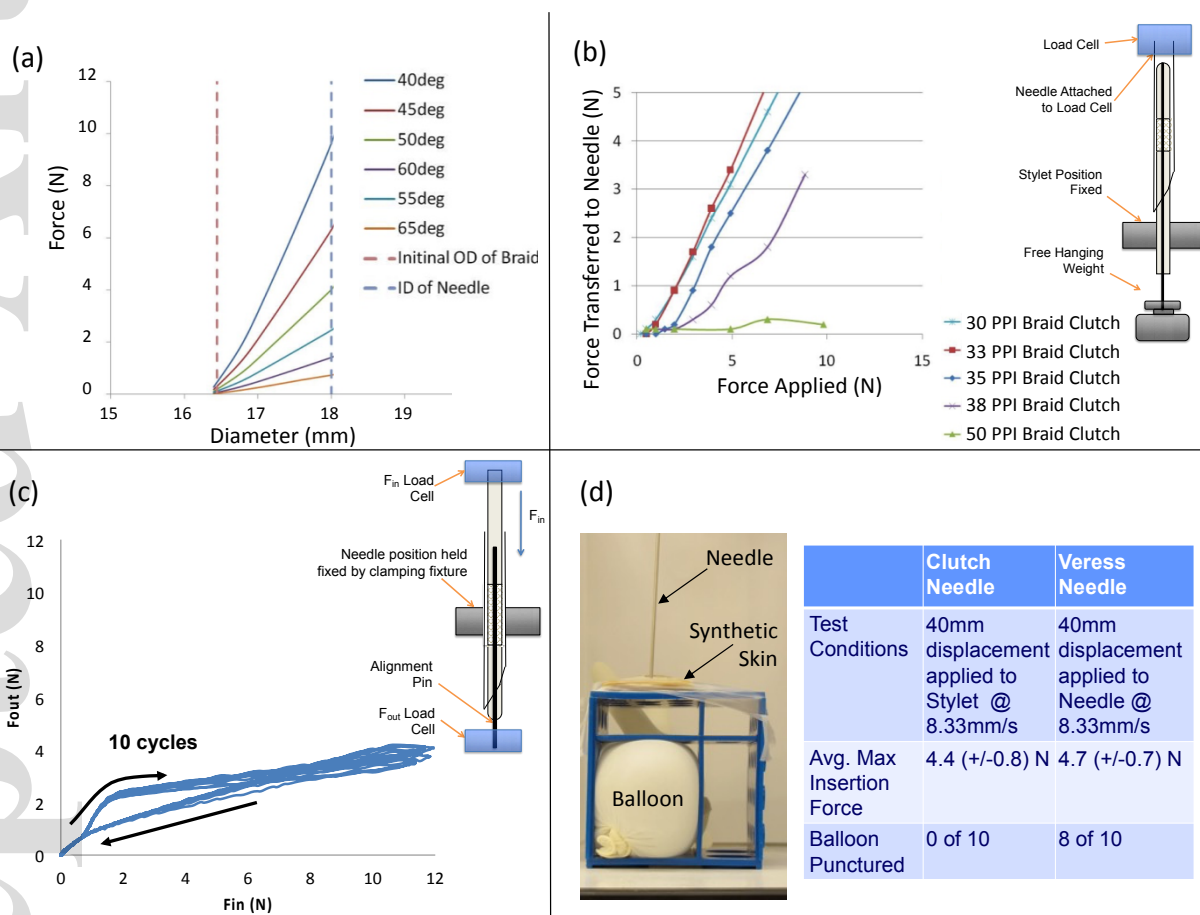


**Figure 3: Design Optimization** (a) Theoretical prediction, adapted from Jedwab et al. [32], of the relative behaviour of radial clutches (initial angle  $\beta$  specified in legend) as they expand from their initial outside diameter (OD) until they contact the inner diameter (ID) of the needle, in response to the application of axial force to the stylet; (b) Experimental demonstration of tunability of the radial clutch. A radial clutch stylet is inverted, its proximal end fixed and its distal end attached to free hanging weights (equivalent force value recorded on x-axis as 'Force Applied'). A load cell is used to record the corresponding force transferred to the needle for increasingly dense braid

*samples, from ~30 PPI to ~50 PPI; (c) Experimental set-up, adapted from Bassett et al. [29], demonstrating the elasticity and repeatability of the clutch engagement mechanism through cyclic loading. The needle is fixed in position and the proximal end of the stylet is connected to one load cell. The input force ( $F_{in}$ ) upon simulating pushing of the stylet is compared to the output force ( $F_{out}$ ) measured by a second load cell at the distal end of the stylet through 10 cycles; (d) Benchtop comparison against Veress needle, gold-standard for closed laparoscopic access, where an inflated latex balloon represents an underlying organ and Syndaver is used to represent skin. The proximal end of the needle or stylet is attached to a uniaxial mechanical tester with the distal end approximating the synthetic skin. The needle mechanisms are lowered by 40mm at 8.33 mm/s and the peak force of insertion recorded. The balloons are inspected for signs of puncture.*

Finally, to illustrate the versatility of the clutch needle and to examine the clutch performance in the presence of biological fluids and tissues, devices were trialed in a series of ex vivo case studies (**Figure 4**). In a human cadaver, where the abdomen was pre-insufflated with CO<sub>2</sub> for visualization, the clutch needle was successfully deployed through the peritoneum with the needle successfully disengaging from the stylet upon entry (**Figure 4(a), Supplementary Video 1**), providing evidence of suitability for closed laparoscopic access. Mechanical clutch needle insertion was repeated 12 times, with an average needle advancement into the abdominal cavity of 14.8 mm or 10.3mm from the end of the needle bevel (bevel length = 4.5 mm). This compares favorably with average of ~ 22 mm insertion reported in the previous iteration of the mechanical clutch needle [29]. Similarly, a proof of principle for experiment was performed on an ex vivo adult porcine model (Adult Yorkshire pig, CBSset, MA, USA) of emergency airway access (**Figure 4(b), Supplementary Video 2**). Here, through endoscopic visualization, the clutch needle can be visualized entering the trachea, but again the needle stops before hitting the back wall and risking tracheal or vocal cord damage. Finally, access of a porcine ear vein (a recently sacrificed adult Yorkshire pig which had been used in an unrelated study, Pine Acres, MA, USA) is used to illustrate the applicability of this device for safe vascular access without the risk of through-puncture injury (**Figure 4(c), Supplementary Video 3**). It is worth noting that these studies were carried out in ex vivo models and further de-risking of the technology will be required in future in vivo experimentation. Testing of prototype devices was confined to 14 and 15 Ga needles, due to a



lack of availability of suitable braids with an appropriate PPI count at smaller diameters, however we believe that the stylet-mounted clutch mechanism described herein is eminently scalable and would also be suitable for use with smaller gauge needles.

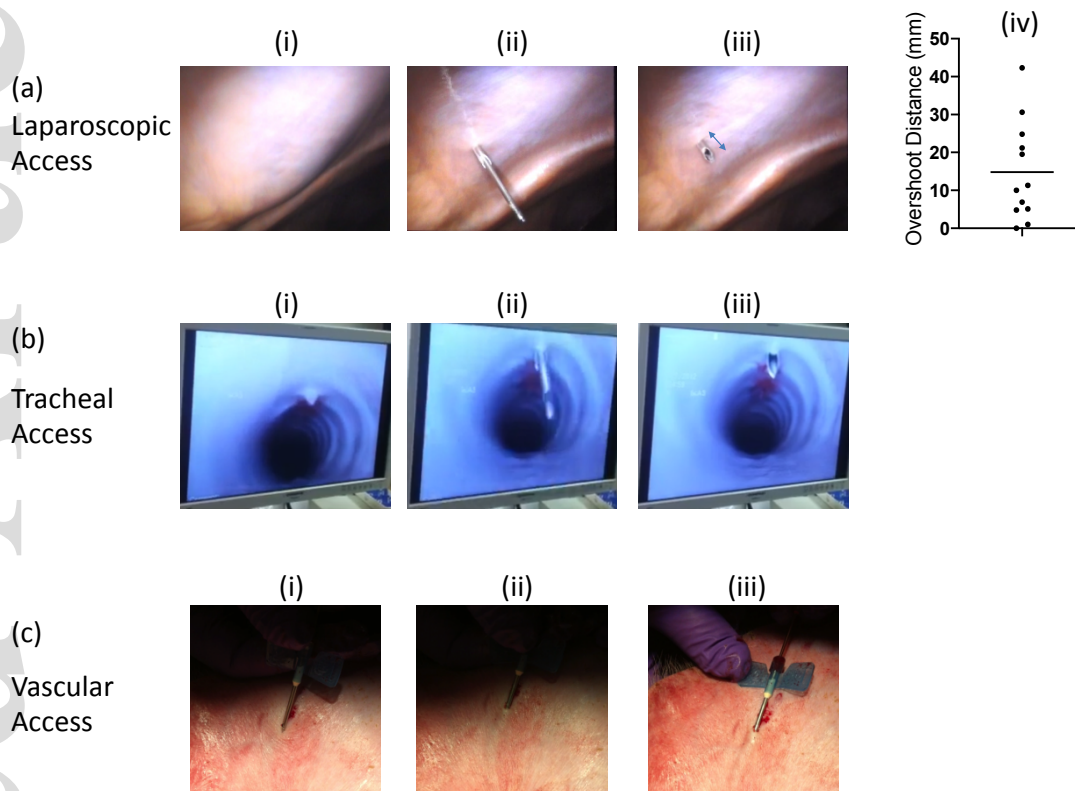


*Figure 4: Proof-of-Concept Pre-clinical assessment of radial clutch needle (a) Laparoscopic Access achieved in a human cadaver with a pre-insufflated abdomen to aid visualization; (b) Tracheal access demonstrated as a means of achieve safe airway access in a porcine model; (c) Vascular access achieved in a porcine ear vein. Still images in each case show (i) tissue tenting prior to needle perforation, (ii) disengagement of radial clutch of blunt stylet (iii) stylet is removed and safe insertion of the needle into target cavity demonstrated. In the case of (a) laparoscopic access, (iv) the overshoot distance was estimated from 12 repeat insertions (line represents mean value).*

In summary, a radial clutch system has been developed and demonstrated initial proof-of-concept functionality in multiple test cases, achieving safe and facile minimally invasive access to

compartments in the body. The radial clutch needle is intuitive to use, which should aid in its clinical adoption. Importantly, the clutch is mounted to a stylet and is inexpensive to manufacture, meaning that is compatible and scalable with procedures where needles are used, irrespective of their gauge size.

## Experimental Section

*Clutch Needle Fabrication:* For bench top and *in vivo* testing, prototypes were assembled using components from disassembled 14Ga Veress Needles (Ranfac, MA), namely a 100mm needle, and 80mm and 50mm proximal and distal stylet segments respectively), coupled with 16 biaxial arranged flat wires (0.051 X 0.127mm, stainless steel 304V) braided over a 1.10mm mandrel, produced by MicroLumen (Florida, USA) with a range of PPI counts (except for the scaled-down 15Ga version used in vascular access testing (**Figure 4(c)**), which comprised a disassembled 15Ga dialysis needle (NxStage Medical Inc, USA)). Segments of braid were initially roughly cut-to-length (~55mm). The ends of the braid were crimped and annealed to avoid unraveling of the braid and to facilitate ease-of-assembly. Braid segments were fixtured and stretched axially before locally heating the ends of the braid with a naked flame **Figure 2(b)** and subsequently being cut-to-length (target length of 40mm). The braid segment was coupled with proximal and distal components of the stylet with an exposed braid length of 15 mm and crimped in-place using a hand crimping tool (DMC AF8 Adjustable Crimp Tool), where the position of the crimps was optimized to maximize retention strength and to minimize the profile of the stylet. Optionally, a Tuohy Borst adapter (Qosina, USA), which contains an adjustable hemostatic valve, was glued to the proximal end to the needle to act as a needle hub and to temporarily couple the stylet to the needle. This facilitated ease of handling and control over the relative position of the needle and stylet prior to activation of the clutch system.

*Theoretical Clutch Performance:* The input force v. diameter relationship in the clutch is governed by equation 1,

$$F = n \left[ \frac{G I_p \cos \beta}{R} \left( \frac{2 \sin \beta \cos \beta}{R} - \frac{2 \sin \beta_0 \cos \beta_0}{R_0} \right) - \frac{E I \sin \beta}{R} \left( \frac{2 \cos^2 \beta}{R} - \frac{2 \cos^2 \beta_0}{R_0} \right) \right] \quad (1)$$



where  $F$  is the axial force exerted on the stylet,  $n$  (number of wires) = 16,  $G$  (shear modulus of the material) = 81.5 GPa,  $I_p$  (polar moment of inertia) =  $\frac{bh}{3}(b^2 + h^2)$ , where  $b = 1.3 \times 10^{-4}$  m &  $h = 5 \times 10^{-5}$  m,  $\beta_0$  (initial angle of the braid wires) = values from  $40^\circ$  to  $65^\circ$ ,  $\beta$  = instantaneous angle of the braid wires,  $R_0$  (initial radius of the braided body) =  $7 \times 10^{-4}$  m,  $R$  = instantaneous radius of the braided body.

#### *Clutch Sensitivity Experiments:*

Clutch sensitivity experiments were performed using an eXpert 7600 mechanical tester (10 N load cell, ADMET, Norwood, MA, USA). The position of the clutch stylet, inverted in the needle, was fixed through coupling to a pin vice on an adjustable y-axis linear rail slide. Similarly, the needle position was fixed to the load cell using a pin vice. Inextensible stainless steel wire was attached to the distal end of the clutch stylet from which a series of free hanging weights was attached (force applied). For 5 clutch stylets of increasing PICC, weights of up to 1kg were added and the corresponding force transferred to the needle recorded from the load cell.

*Repeatability of Clutch Engagement Experiments:* Using an experimental set up similar to Bassett et al., [29], a custom dual-load-cell set-up was developed to record both input and output forces within the system. In this instance, the needle was fixed to the adjustable y-axis slider, while the stylet was mounted to the load cell (25N, Admet). An alignment pin was used to preserve the perpendicularity of the distal end of the stylet to the output force load cell (10N, Admet). The stylet was cycled (10 cycles) at a constant rate of displacement up to an application force of 12N and the corresponding output force recorded.

*Simulated Use Benchtop Testing:* A benchtop model was used to simulate closed laparoscopic access and offer a side-by-side comparison of the clutch needle versus the Veress needle (Ranfac, USA). The model comprised of synthetic skin (Syndaver, USA) placed on top of a test tube rack, with a latex balloon used to simulate an organ or tissue sensitive to damage lying ~20mm under the tissue surface. To simulate insertion, the needles were placed in the mechanical tester and the needle (Veress) or stylet (Clutch device) was displaced by 40mm (at a speed of 8.33 mm/s) until the synthetic tissue was punctured. The latex balloon was inspected for damage and the maximum insertion force into the synthetic skin was recorded.

*Pre-clinical Proof-of-principle Testing:* The assembled devices were assessed in a series of simulated clinical scenarios for proof of concept testing. Firstly, in a fresh human cadaver (Massachusetts General Hospital), a sample clutch needle was inserted into the peritoneum and recorded through a laparoscopic camera. Pre-insufflation of the abdomen with CO<sub>2</sub> was used to improve visualization of the field of insertion. The distance that the needle inserted into the peritoneum was estimated from still images of 12 independent insertions. Secondly, emergency airway access was simulated by needle insertion into a pig trachea and visualized using a gastroscopic camera. Finally, the potential utility of the clutch needle in vascular access was demonstrated by insertion into the ear vein of an adult pig, which had been recently sacrificed.

### Acknowledgements

Funding for this research was provided by the Wallace H. Coulter Foundation (WCF0121TN) and an NIH R01 grant (HL095722) to JMK. The authors would like to acknowledge Richard Gedney for the support in customization of Admet's mechanical testing equipment.

Received: ((will be filled in by the editorial staff))

Revised: ((will be filled in by the editorial staff))

Published online: ((will be filled in by the editorial staff))

### References

1. Smith, E.H., *Complications of Percutaneous Abdominal Fine-Needle Biopsy - Review*. Radiology, 1991. **178**(1): p. 253-258.
2. Stone, N.N. and R.G. Stock, *Complications following permanent prostate brachytherapy*. European Urology, 2002. **41**(4): p. 427-433.
3. Mcneill, M.J. and J. Thorburn, *Cannulation of the Epidural Space*. Anaesthesia, 1988. **43**(2): p. 154-155.

4. Selander, D., K.G. Dhuner, and G. Lundborg, *Peripheral-Nerve Injury Due to Injection Needles Used for Regional Anesthesia - Experimental-Study of Acute Effects of Needle Point Trauma*. Acta Anaesthesiologica Scandinavica, 1977. **21**(3): p. 182-188.
5. Mignatti, A., P. Friedmann, and D.P. Slovit, *Targeting the safe zone: A quality improvement project to reduce vascular access complications*. Catheterization and Cardiovascular Interventions, 2018. **91**(1): p. 27-32.
6. Di Iorio, B.R., et al., *Vascular access for hemodialysis: The impact on morbidity and mortality*. Journal of Nephrology, 2004. **17**(1): p. 19-25.
7. Okeson, G.C. and P.H. Wulbrecht, *The safety of brachial artery puncture for arterial blood sampling*. Chest, 1998. **114**(3): p. 748-751.
8. Jackson, D.W., N.A. Evans, and B.M. Thomas, *Accuracy of needle placement into the intra-articular space of the knee - Reply*. Journal of Bone and Joint Surgery-American Volume, 2004. **86a**(2): p. 434-434.
9. Schafer, M., M. Lauper, and L. Krahenbuhl, *Trocar and Veress needle injuries during laparoscopy*. Surgical Endoscopy-Ultrasound and Interventional Techniques, 2001. **15**(3): p. 275-280.
10. Champault, G., F. Cazacu, and N. Taffinder, *Serious trocar accidents in laparoscopic surgery: A French survey of 103,852 operations*. Surgical Laparoscopy & Endoscopy, 1996. **6**(5): p. 367-370.
11. Orlando, R., P. Palatini, and F. Lirussi, *Needle and trocar injuries in diagnostic laparoscopy under local anesthesia: What is the true incidence of these complications?* Journal of Laparoendoscopic & Advanced Surgical Techniques-Part A, 2003. **13**(3): p. 181-184.
12. Krishnakumar, S. and P. Tambe, *Entry complications in laparoscopic surgery*. Journal of gynecological endoscopy and surgery, 2009. **1**(1): p. 4.
13. Vindal, A. and P. Lal, *The Veress needle causes most laparoscopic injuries and should be abandoned FOR: The open technique is safer and saves time*. Bjog-an International Journal of Obstetrics and Gynaecology, 2015. **122**(1): p. 141-141.
14. Ahmad, G., et al., *Laparoscopic entry techniques*. Cochrane Database Syst Rev, 2015. **8**: p. CD006583.
15. O'Toole, D., et al., *Assessment of complications of EUS-guided fine-needle aspiration*. Gastrointestinal Endoscopy, 2001. **53**(4): p. 470-474.

16. Atallah, S., et al., *Natural-orifice transluminal endoscopic surgery*. British Journal of Surgery, 2015. **102**(2): p. E73-E92.
17. Rynd, F., *Neuralgia—introduction of fluid to the nerve*. Dublin Med Press, 1845. **13**(167): p. 19.
18. Moureau, N., et al., *Evidence-based consensus on the insertion of central venous access devices: definition of minimal requirements for training*. Br J Anaesth, 2013. **110**(3): p. 347-56.
19. Abolhassani, N., R. Patel, and M. Moallem, *Needle insertion into soft tissue: A survey*. Medical Engineering & Physics, 2007. **29**(4): p. 413-431.
20. van Gerwen, D.J., J. Dankelman, and J.J. van den Dobbelsteen, *Needle-tissue interaction forces - A survey of experimental data*. Medical Engineering & Physics, 2012. **34**(6): p. 665-680.
21. Hiemenz, L., A. Litsky, and P. Schmalbrock. *Puncture mechanics for the insertion of an epidural needle*. in *Americal Society of Biomechanics 21th Annual Meeting*. 1997.
22. Podder, T.K., et al., *Evaluation of robotic needle insertion in conjunction with in vivo manual insertion in the operating room*. 2005 Ieee International Workshop on Robot and Human Interactive Communication (Ro-Man), 2005: p. 66-72.
23. Podder, T., et al., *In vivo motion and force measurement of surgical needle intervention during prostate brachytherapy*. Medical physics, 2006. **33**(8): p. 2915-2922.
24. Chitnis, G.D., et al., *A resistance-sensing mechanical injector for the precise delivery of liquids to target tissue*. Nature Biomedical Engineering, 2019: p. 1 %@ 2157-846X.
25. Begg, N.D.M., *Increasing the safety and precision of medical tissue puncture*. 2014, Massachusetts Institute of Technology.
26. Nevler, A., et al., *Safer trocar insertion for closed laparoscopic access: ex vivo assessment of an improved Veress needle*. Surgical Endoscopy and Other Interventional Techniques, 2016. **30**(2): p. 779-782.
27. Leibinger, A., M.J. Oldfield, and F.R.Y. Baena, *Minimally disruptive needle insertion: a biologically inspired solution*. Interface Focus, 2016. **6**(3).
28. Song, D.Y., et al., *Robotic needle guide for prostate brachytherapy: Clinical testing of feasibility and performance*. Brachytherapy, 2011. **10**(1): p. 57-63.
29. Bassett, E.K., et al., *Design of a mechanical clutch-based needle-insertion device*. Proc Natl Acad Sci U S A, 2009. **106**(14): p. 5540-5.

- Accepted Article
30. Stoeckel, D., A. Pelton, and T. Duerig, *Self-expanding nitinol stents: material and design considerations*. *European Radiology*, 2004. **14**(2): p. 292-301.
  31. Feins, E.N., et al., *A growth-accommodating implant for paediatric applications*. *Nature Biomedical Engineering*, 2017. **1**(10): p. 818-825.
  32. Jedwab, M.R. and C.O. Clerc, *A Study of the Geometrical and Mechanical-Properties of a Self-Expanding Metallic Stent Theory and Experiment*. *Journal of Applied Biomaterials*, 1993. **4**(1): p. 77-85.
  33. Wahl, A., *Mechanical springs, 1963*. McGAWHILL, p119.